

Two-Dimensional Dynamic-Director ¹³C NMR of Liquid Crystals

Dan McElheny, Min Zhou, and Lucio Frydman¹

Department of Chemistry (M/C 111), University of Illinois at Chicago, 845 W. Taylor Street, Chicago, Illinois 60607-7061

Received May 30, 2000; revised November 6, 2000

A novel nuclear magnetic resonance (NMR) experiment for facilitating the resolution and assignment of liquid crystalline ¹³C NMR spectra is described. The method involves the motor-driven reorientation of the liquid crystalline director, in synchrony with the acquisition of a 2D chemical shift correlation spectrum. By monitoring in this fashion the ¹³C NMR evolution of spins in the liquid crystal at two different director orientations with respect to the magnetic field, the method distinguishes anisotropic from isotropic displacements and can be utilized for assigning the resonances and estimating local degrees of order. Of various potential pairs of angles suitable for such a correlation, the (0°, 90°) choice was found to be most convenient, as it avoids line broadening complications that may otherwise originate from heterogeneities of the oriented phase. The technique thus derived was employed in the analysis of a series of monomeric and polymeric liquid crystal systems. © 2001 Academic Press

Key Words: mesophases; two-dimensional NMR; ¹³C chemical shift correlations; spin anisotropies; liquid crystalline polymers.

Valuable orientational, dynamic, and structural insight on the nature of a liquid crystal (LC) and of solutes that are dissolved in it can in principle be extracted from nuclear magnetic resonance (NMR) spectra recorded on such phases oriented inside the main magnetic field (1–5). A precondition to be fulfilled by these data, however, is that they need to be simple enough to be amenable to analysis. Interactions and Hamiltonians in mesophases are characterized by only a partial averaging of the anisotropic spin couplings, thereby leading to NMR spectra that tend to be significantly more complex than those from their isotropic liquid counterparts. When dealing with natural abundance spin probes, spectral intractability tends to be the norm if observations are made on extensively coupled networks such as multiple nearby protons, but not when spectra are acquired on dilute low- γ nuclei like ¹³C. Such traces will generally exhibit sharp resonances under efficient ¹H decoupling conditions, whose positions depend on the chemical nature of each site (defining the isotropic chemical shift contribution) as well as on the site's degree of ordering in the LC phase (affecting the anisotropic displacement).

¹ To whom correspondence should be addressed at Department of Chemistry (M/C 111), University of Illinois at Chicago, 845 W. Taylor Street, Room 4500, Chicago, IL 60607-7061. Fax: (312) 996-0431. E-mail: lucio@samson.chem.uic.edu.

These features have recently been exploited in ¹³C NMR investigations on the order and dynamics adopted by certain aromatic polyamides prone to mesophase formation (6–8). Main chain polymers of this kind can lead to anisotropic fluids when dissolved at appropriate concentrations (9–13); macromolecules are then susceptible to orientation by external shear forces and when coagulated will yield solid fibers with several remarkable material properties including strength, heat stability, and chemical resistance (9, 14, 15). During the course of such studies, we have encountered a number of spectral assignment challenges known to characterize liquid crystalline ¹³C NMR analyses in general. These stem from the fact that the common chemical shift criteria on which the assignment of ¹³C peaks in organic molecules are based, which compare the resonances' isotropic positions δ_{iso} with tabulated values, are of limited use in anisotropic phases where magnetically induced alignment can bring *a priori* unknown shifts of the resonances into play. Among the most successful methods that have been hitherto developed to cope with these assignment problems is the variable-angle-spinning (VAS) experiment, which relies on spinning LC samples rapidly enough at an angle θ with respect to the magnetic field B_0 (16–19). For sufficiently nonviscous phases and within a certain range of spinning angles this procedure aligns the LC director parallel to the macroscopic axis of rotation; rapid molecular tumbling will then shift peaks in the ¹³C NMR spectra to new chemical shifts, δ_{obs} , characterized by

$$\delta_{\text{obs}} = \delta_{\text{iso}} + \delta_{\text{aniso}} \cdot P_2(\cos \theta),$$

where δ_{aniso} is the anisotropic displacement exhibited by a site in the LC phase and $P_2(\cos \theta) = (3 \cos^2 \theta - 1)/2$. Angular manipulations of the director orientation with respect to the magnetic field enable these VAS experiments to discriminate between the isotropic and anisotropic contributions to a peak's chemical shift δ_{obs} , yielding the nature of the chemical site via the former contribution plus information about the LC order via the δ_{aniso} parameter.

When the molecular weight of the mesogen increases or the LC transitions from a nematic to a more ordered type of arrangement (as in the case of LC polymers or in smectics), spinning-induced alignment becomes ineffective and the use-

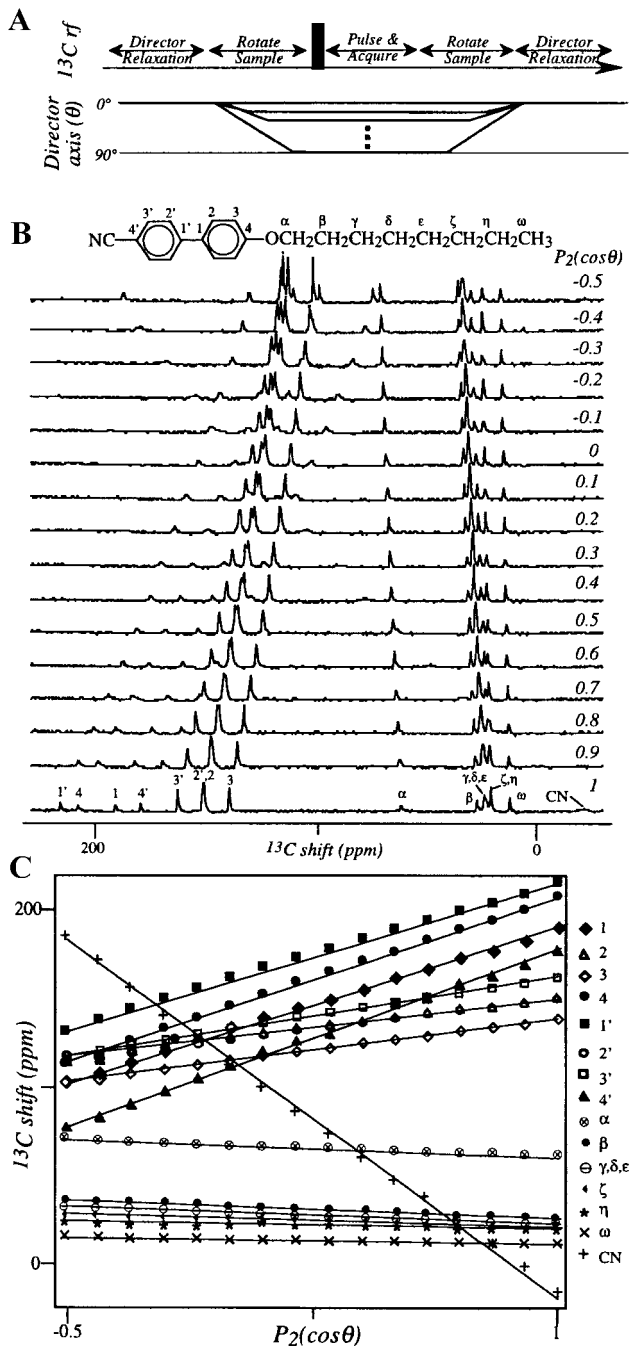


FIG. 1. (A) 1D variable director approach to the assignment of resonances in liquid crystal ^{13}C NMR. The experiment involves an initial equilibration period, a reorientation of the sample with respect to B_0 in combination with the NMR data acquisition, and a return of the LC director to its equilibrium position prior to the following scan. (B) Variable director ^{13}C NMR spectra of 4-*n*-octyloxy-4'-cyanobiphenyl (8OCB) in its smectic S_A phase, collected at the indicated $P_2(\cos\theta)$ values with respect to B_0 . These experiments were carried out at 4.7 T on a laboratory-built doubly tuned NMR spectrometer and probe, using a $5\text{-}\mu\text{s}$ $\pi/2$ ^{13}C excitation pulse and heteronuclear decoupling with fields of 70 kHz. LC directors throughout these experiments were rotated away from equilibrium inside a static radiofrequency solenoid coil positioned perpendicular to B_0 , using a string-driven pulley rotating a coaxial 5-mm-OD glass container. The pulley was interphased to a Whedco, Inc., motor and controller system driven in turn by the spectrometer's pulse programmer. A

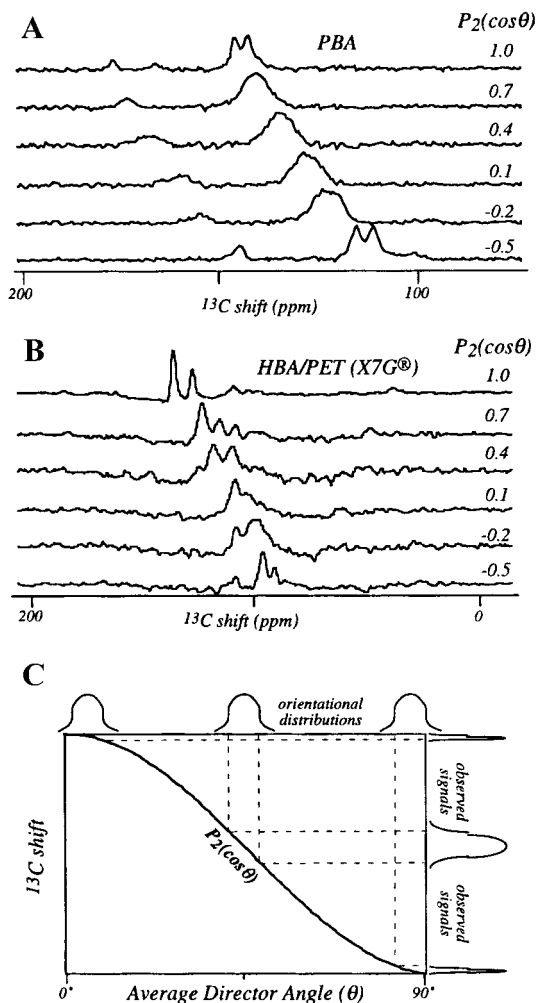


FIG. 2. (A) Variable-director ^{13}C NMR spectra collected on a 14% w/w PBA/ H_2SO_4 solution at room temperature and at the indicated $P_2(\cos\theta)$ values. Experimental conditions were similar to those in Fig. 1, except that 4000 scans per spectrum were used. (B) Variable-director ^{13}C NMR spectra were collected on the commercial *p*-hydroxybenzoic acid/*p*-ethyleneterephthalate thermotropic copolymer X7G (Eastman). Experimental conditions were similar to those in (A), but data were collected on the neat molten polyester at 200°C . (C) Rationalization of the resonance line broadening observed for the LC polymers as a function of orientation with respect to B_0 : whereas perfectly aligned systems (possessing very sharp θ distributions) or fast-reorienting ones (capable of sampling a range of θ values rapidly on the NMR time scale) will only show a linear $P_2(\cos\theta)$ shift as a function of θ , slowly reorienting distributions will also display a partly averaged powder lineshape reflecting the distribution of molecular orientations. When these distributions are centered at $\theta = 0^\circ$ or 90° the observable signals narrow.

total of 512 scans with a 2-s recycle delay were recorded for each spectrum. Temperature was set at 52°C using a gas stream warmed with a laboratory-built system controlled by Omega, Inc., components; other than for a reduced duty cycle ($\leq 1\%$), no special precautions were taken for compensating for potential RF heating. (C) Linear dependencies observed for the chemical shifts of the various ^{13}C sites of 8OCB as a function of $P_2(\cos\theta)$; the best fit lines reveal each site's isotropic shift and, with it, their chemical nature.

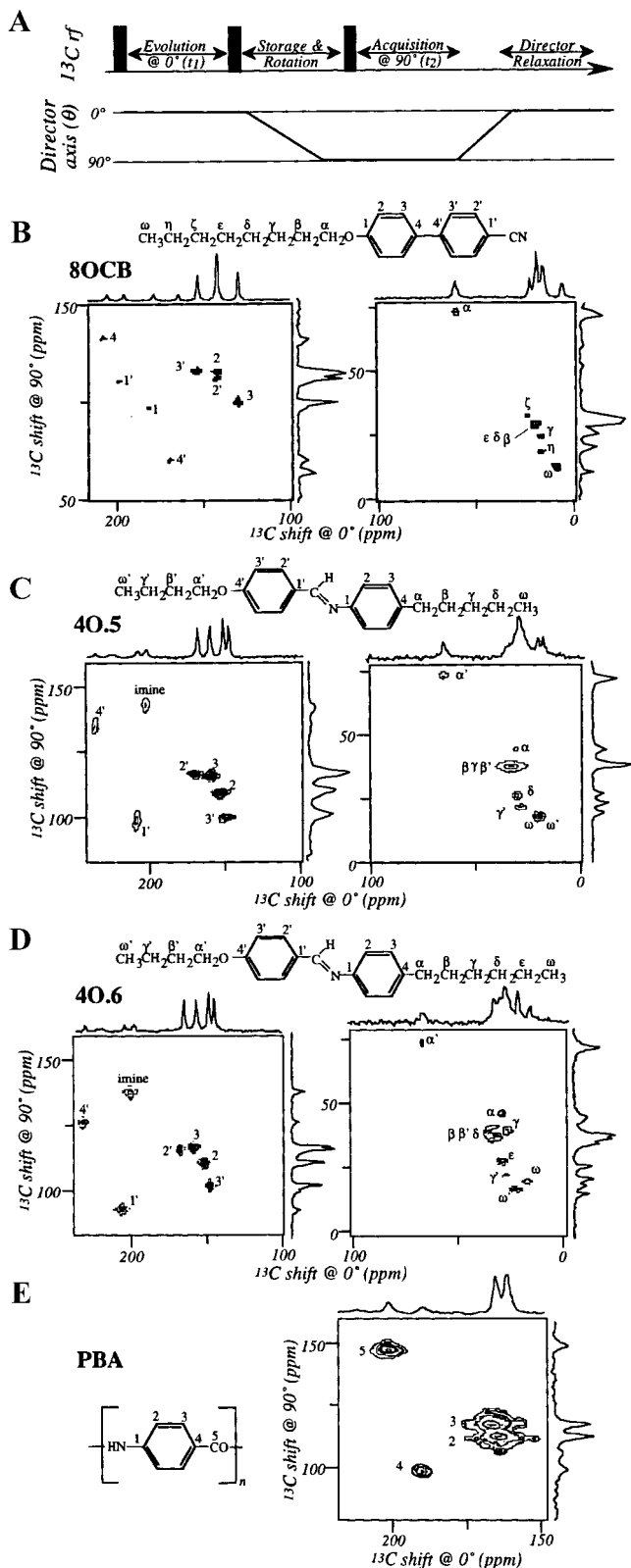


FIG. 3. (A) General strategy involved in the $0^\circ/90^\circ$ 2D dynamic-director correlation experiment; thick bars indicate $\pi/2$ pulses, and further details are presented in the text. (B–E) 2D dynamic-director correlation spectra observed for the various indicated compounds. Hardware and acquisition parameters

fulness of this VAS approach is compromised. For dealing with such situations we have recently proposed a variable-director protocol which allows for the discrimination between the isotropic and the anisotropic contributions to a particular ^{13}C resonance, but which does not rely on a spinning-induced reorientation of the LC director (20). Scaling of spin anisotropies is achieved in these experiments by exploiting the higher viscosities of the LC phases, which enable changing the orientation of the director away from its equilibrium position simply with the aid of a rigid-body reorientation. Driven by a stepping motor, the sample can thus be kept in a nonequilibrium state $\theta \neq 0^\circ$ while a ^{13}C NMR scan is recorded, then mechanically rotated back to its equilibrium position parallel to B_0 and kept there during the relaxation delay until the procedure is repeated (Fig. 1A). Figure 1B shows an application of this approach to the smectic phase of 80CB, a low-molecular-weight LC for which director relaxation times at these temperatures are in the 10^0 - to 10^1 -s regime. These allow us to acquire variable-director NMR spectra using off-equilibrium acquisition and on-equilibrium relaxation times in the order of 10^{-2} and 1 s, respectively; a complete $0^\circ < \theta < 180^\circ$ angular range of director orientations can thus be explored and from these individual isotropic and anisotropic coupling contributions to the peaks' displacements extracted via a simple linear analysis of the data (Fig. 1C).

During the course of subsequent investigations we found that such a protocol, even though applicable to moderately viscous monomeric and polymeric LCs, ceases to be significantly helpful when dealing with large macromolecular assemblies. Figure 2A, for instance, illustrates some of the results that we have observed when ^{13}C variable-director NMR spectra were collected on a solution of the high-strength aramide polymer poly(*p*-benzamide) (PBA) dissolved in concentrated (100.4%) sulfuric acid. Contrary to what was observed on the monomeric smectics or on the relatively low M_w thermotropic polymers that were previously investigated (20), ^{13}C NMR signals in these spectra no longer undergo a simple change in their chemical shift positions as a function of θ . They also experience a significant broadening. This type of behavior was observed in all of the lyotropic aramide solutions that we studied, as well as in certain types of commercial high M_w thermotropic polyesters (Fig. 2B). By preventing a clear iden-

similar to those described in Figs. 1 and 2 were utilized in these experiments; 128 t_1 points were acquired to obtain each of the 2D smectic spectra, whereas 32 t_1 points sufficed for the PBA acquisition. Data for *p*-butoxybenzylidene-*p*-pentylaniline (40.5) and *p*-butoxybenzylidene-*p*-hexylaniline (40.6) were acquired at 48°C , where both compounds exhibit smectic phases. Aromatic and aliphatic regions for 80CB, 40.5, and 40.6 are shown separated to better illustrate the resolution introduced by the experiment. Using the chemical shift displacements observed for each resonance along the two spectral axes of these experiments the isotropic frequency of each LC resonance could be calculated (Table 1); these peaks were assigned as indicated by comparison to previous assignments of the isotropic-phase spectra reported in the literature (30, 31).

TABLE 1
Comparison between ^{13}C Shifts Observed for the Indicated Sites by 2D Dynamic-Director LC Experiments
and the Corresponding Isotropic-Phase ^{13}C NMR Shifts

	80CB																CN	
	1	2	3	4	1'	2'	3'	4'	α	β	γ	δ	ϵ	ζ	η	ω		
$\delta_{\text{obs}}(\text{LC}, 0^\circ)^a$	188.6	149.5	138.0	214.3	205.9	149.5	161.2	176.4	61.0	22.3	19.4	22.3	22.3	25.7	18.9	10.1	<i>m</i>	
$\delta_{\text{obs}}(\text{LC}, 90^\circ)^a$	99.4	115.6	102.3	131.4	111.1	113.2	116.6	75.5	67.5	32.0	28.6	32.0	32.0	34.1	23.6	14.7	<i>m</i>	
$\delta_{\text{iso}}(\text{LC})^b$	129.1	126.7	114.2	159.0	142.7	125.3	131.5	109.3	67.5	28.8	25.5	28.8	28.8	31.3	22.0	13.2	<i>m</i>	
$\delta_{\text{iso}}(\text{iso})^c$	130.6	127.8	115.1	159.8	144.3	126.4	132.1	110.1	68.2	29.4	26.0	29.4	29.4	31.8	22.5	13.8	118.4	
40.5																		
	1	2	3	4	1'	2'	3'	4'	α	β	γ	δ	ω	α'	β'	γ'	ω'	Imine
$\delta_{\text{obs}}(\text{LC}, 0^\circ)^d$	<i>m</i>	150.0	158.4	207.7	<i>m</i>	167.2	145.9	201.8	27.0	22.2	22.2	21.0	10.3	60.9	22.2	18.6	7.3	227.3
$\delta_{\text{obs}}(\text{LC}, 90^\circ)^d$	<i>m</i>	113.0	118.7	103.0	<i>m</i>	118.6	104.3	143.2	35.5	35.4	35.4	23.9	15.9	70.4	35.4	20.3	17.4	120.0
$\delta_{\text{iso}}(\text{LC})^e$	<i>m</i>	125.3	131.9	137.9	<i>m</i>	134.8	118.2	162.7	32.6	31.0	31.0	22.9	14.0	67.4	31.0	19.7	14.0	155.8
$\delta_{\text{iso}}(\text{iso})^f$	150.6	121.7	131.9	140.5	131.1	131.1	118.1	162.7	36.4	32.7	32.7	23.4	14.9	68.7	32.7	20.2	14.9	158.0
40.6																		
	1	2	3	4	1'	2'	3'	4'	α	β/δ	γ	ϵ	ω	α'	β'	γ'	ω'	Imine
$\delta_{\text{obs}}(\text{LC}, 0^\circ)^g$	<i>m</i>	150.0	158.3	225.9	167.2	208.2	145.9	236.8	26.9	25.1	25.7	19.8	7.3	61.4	25.1	18.6	13.2	201.7
$\delta_{\text{obs}}(\text{LC}, 90^\circ)^g$	<i>m</i>	108.5	114.4	97.4	113.4	90.2	99.5	124.0	38.1	36.6	34.7	26.0	18.7	71.3	36.6	21.1	15.6	135.5
$\delta_{\text{iso}}(\text{LC})^h$	<i>m</i>	122.3	129.1	140.2	131.3	129.6	115.0	161.6	34.4	32.8	31.6	23.9	14.9	68.0	32.8	20.3	14.8	157.6
$\delta_{\text{iso}}(\text{iso})^i$	150.5	121.6	129.7	140.0	130.8	130.8	115.1	162.2	36.3	32.3	29.9	23.5	14.6	68.5	32.3	19.9	14.6	157.7
PBA																		
	1		2		3		4		5									
$\delta_{\text{obs}}(\text{LC}, 0^\circ)^j$	<i>m</i>		158.1		163.0		192.2		206.9									
$\delta_{\text{obs}}(\text{LC}, 90^\circ)^j$	<i>m</i>		110.7		117.2		102.2		157.2									
$\delta_{\text{iso}}(\text{LC})^k$	<i>m</i>		126.5		132.5		141.3		173.7									
$\delta_{\text{iso}}(\text{iso})^l$	134.2		125.7		131.5		139.6		173.2									

^a From Fig. 3B.

^b Isotropic chemical shifts calculated from LC data (52°C); ± 0.5 ppm.

^c Measured in the isotropic melt (67°C).

^d From Fig. 3C.

^e Isotropic chemical shifts calculated from LC data (48°C); ± 0.5 ppm.

^f Measured in the isotropic melt (80°C).

^g From Fig. 3D.

^h Isotropic chemical shifts calculated from LC data (48°C); ± 0.5 ppm.

ⁱ Measured in the isotropic melt (80°C).

^j From Fig. 3E.

^k Isotropic chemical shifts calculated from LC data (25°C); ± 0.5 ppm.

^l Measured in the isotropic solution (25°C).

^m Missing or ambiguous due to poor signal/noise ratio.

tification of the individual peaks over the full angular range, such broadenings deprive the variable-director approach from much of its spectral assignment usefulness. Similar broadenings have in fact been reported in variable-director EPR and ^1H NMR experiments of certain frozen-like ordered networks including smectics, cholesterics, and membranes (21–24). Their origin can be traced to the distribution in orientations that actually characterizes molecules within the LC phase and

which when coupled to a slow rate of molecular tumbling prevents anisotropic tensors from leading to sharp, exchange-narrowed lineshapes. Rather than introducing a conventional displacement of the anisotropic ^{13}C resonances, the incomplete alignment that characterizes LC samples originates then a “powder-like” lineshape for each inequivalent site (Fig. 2C).

Valuable details can be learned about the order and dynamics of polymeric LC phases from a detailed analysis of these

variable-director lineshapes (25). For the purposes of the present study, however, the point to remark is that, given the $P_2(\cos \theta)$ -type scaling of the shielding anisotropies, there will generally be two LC director orientations with respect to B_0 for which well-resolved peaks can be observed: $\theta = 0^\circ$ and $\theta = 90^\circ$. This is a consequence of the slow angular dependencies that characterize the dispersion in coupling anisotropies at these extrema of $P_2(\cos \theta)$, and it motivated us to explore an alternative route for obtaining isotropic ^{13}C chemical shift information from LC samples based on making correlated 2D NMR observations at such angles. The pulse sequence that results is akin to that of 2D exchange-type experiments recently proposed for studying couplings and orientations in solids (26–29); it involves an initial evolution time t_1 during which the LC director is held parallel to B_0 , a storage period during which the sample is rapidly (≈ 50 ms) reoriented away from equilibrium and an acquisition time in which the sample's signal is recorded as a function of t_2 at a position $\theta = 90^\circ$ (Fig. 3A). After completing this acquisition the sample is returned back to the $\theta = 0^\circ$ position and the LC director allowed to equilibrate parallel to B_0 in preparation for a new scan. This whole procedure is repeated for various t_1 times until a full 2D $S(t_1, t_2)$ signal is obtained; a conventional phase cycling of the individual pulses then helps retrieve echo and anti-echo data sets from which purely absorptive lineshapes can be calculated. Figures 3B–3E present a series of such 2D dynamic-director spectra, collected for a lyotropic PBA solution as well as for a number of monomeric viscous smectics. All of these compounds showed extensive signal overlap in their conventional ^{13}C LC NMR spectra (at least at the relatively low field strength used in this study) as well as when 1D spectra were acquired at $\theta = 90^\circ$. The correlation at both director orientations, on the other hand, provides a significant resolution enhancement for both aromatic and aliphatic resonances. This site resolution can be traced to the different coordinates defining the peak positions along the two axes of these spectra: $(\delta_{\text{iso}} + \delta_{\text{aniso}})$ for $\theta = 0^\circ$ and $(\delta_{\text{iso}} - \delta_{\text{aniso}}/2)$ for $\theta = 90^\circ$. From these positions a simple computation enables the calculation of the isotropic chemical shifts for each LC resonance and then, by comparisons with chemical shift tables or with isotropic-phase assignments, an identification of the chemical sites that originate them.

Table 1 presents such an analysis for the various compounds whose spectral analysis is illustrated in Fig. 3. This table also presents a comparison between the isotropic chemical shift characterizing each site in the isotropic phase, with the isotropic shielding that characterizes such sites in the LC fluid. Interestingly, there seem to be only minor and mostly nonsystematic differences between both sets of isotropic shifts. For the aliphatic chains of the smectic molecules these are almost within the experimental error, suggesting that such residues undergo very modest changes in their average conformations upon going from the ordered to the disordered phases. Somewhat unexpectedly, the largest variations are exhibited by

certain aromatic sites, hinting at steric or π -conjugation changes as these molecules undergo the LC \leftrightarrow isotropic phase transition. The absence of systematic peak shifts as all compounds go from a liquid crystalline to an isotropic phase is also suggestive of minor changes in the isotropic magnetic susceptibility of the samples; anisotropic susceptibility contributions transform as $P_2(\cos \theta)$ and thus are beyond the protocol's ability to differentiate them from shielding anisotropies.

These initial results illustrate the potential usefulness of 2D dynamic-director NMR techniques to enhance the resolution and facilitate the assignment of ^{13}C LC spectra. The method is relatively simple and thus applicable even under extreme temperature conditions; its only technical requirement is the interphasing of the sample to a stepping motor, and it is applicable to any LC system whose director relaxation times are sufficiently long to enable data acquisition off-equilibrium. Yet when compared with the variable-director approach illustrated in Fig. 1, the 2D $0^\circ/90^\circ$ dynamic-director procedure suffers from a number of disadvantages, including a lengthier overall acquisition time derived from the resolution needs of its indirectly detected dimension and an additional signal-to-noise penalty arising from the intermediate storage period. This latter problem is compounded by the relatively short longitudinal relaxation times that certain ^{13}C sites may have in polymeric or smectic liquid crystals; in fact in all of the compounds that we analyzed there happened to be resonances, always coming from a ^{13}C site bonded to ^{14}N , that appeared in the 1D conventional spectrum but failed to show up in the 2D NMR correlations. Notwithstanding this complication, the information and resolution conveyed by these 2D NMR data provide assistance when trying to analyze spectra in LC systems with orientational heterogeneities, which is unavailable from alternative experiments.

ACKNOWLEDGMENTS

We are grateful to Dr. Veronica Frydman (UIC) for the synthesis and preparation of the PBA samples. This work was supported by the National Science Foundation through Grants DMR-9806810 and CHE-9841790 (Creativity Extension Award). L.F. is a Camille Dreyfus Teacher–Scholar (1996–2001), University of Illinois Junior Scholar (1997–2000), and Alfred P. Sloan Fellow (1997–2000).

REFERENCES

1. P. Diehl and C. L. Khetrpal, "NMR Studies of Molecules Oriented in Nematic Liquid Crystals," Springer-Verlag, New York, 1969.
2. J. W. Emsley and J. C. Lindon, "NMR Spectroscopy Using Liquid Crystal Solvents," Pergamon, Oxford, 1975.
3. J. W. Emsley (Ed.), "NMR of Liquid Crystals," Reidel, Dordrecht, 1985.
4. R. Y. Dong, "Nuclear Magnetic Resonance of Liquid Crystals," Springer-Verlag, New York, 1994.
5. G. R. Luckhurst and C. A. Veracini (Eds.), "The Molecular Dynamics of Liquid Crystals," Kluwer, Dordrecht, 1994.

6. M. Zhou, V. Frydman, and L. Frydman, *J. Phys. Chem.* **100**, 19280 (1996).
7. M. Zhou, V. Frydman, and L. Frydman, *Macromolecules* **30**, 5416 (1997).
8. D. McElheny, V. Frydman, M. Zhou, and L. Frydman, *J. Phys. Chem. A* **103**, 4830 (1999).
9. S. L. Kwolek, P. W. Morgan, J. R. Schaefgen, and L. W. Gulrich, *Macromolecules* **10**, 1390 (1977).
10. E. T. Samulski, *Phys. Today* **35**, 40 (1982).
11. H. Finkelmann, *Angew. Chem. Int. Ed. Engl.* **26**, 816 (1987).
12. V. N. Tsvetkov, "Rigid Chain Polymers," Plenum, New York, 1989.
13. C. Carfagna (Ed.), "Liquid Crystalline Polymers," Pergamon, Oxford, 1994.
14. H. H. Yang, "Aromatic High-Strength Fibers," Wiley, New York, 1989.
15. A. I. Isayev, T. Kyu, and S. Z. D. Cheng (Eds.), "Liquid Crystalline Polymer Systems," ACS, Washington, 1996.
16. J. Courtieu, D. W. Alderman, and D. M. Grant, *J. Am. Chem. Soc.* **103**, 6783 (1981).
17. R. Teeaar, M. Alla, and E. Lippmaa, *Org. Magn. Reson.* **19**, 134 (1982).
18. B. M. Fung and M. Gangoda, *J. Chem. Phys.* **83**, 3285 (1985).
19. J. Courtieu, J. P. Bayle, and B. M. Fung, *Progr. Nucl. Magn. Reson. Spectrosc.* **26**, 141 (1994).
20. M. Zhou, V. Frydman, and L. Frydman, *J. Am. Chem. Soc.* **120**, 2178 (1998).
21. Z. Luz and S. Meiboom, *J. Chem. Phys.* **59**, 275 (1973).
22. E. Meirovitch and J. H. Freed, *J. Phys. Chem.* **88**, 4995 (1984).
23. K. Mueller, P. Meier, and G. Kothe, *Progr. Nucl. Magn. Reson. Spectrosc.* **17**, 211 (1985).
24. C. Glaubitz and A. Watts, *J. Magn. Reson.* **130**, 305 (1998).
25. J. Grinshtein, D. McElheny, V. Frydman, and L. Frydman, *J. Chem. Phys.*, in press.
26. P. M. Henrichs, *Macromolecules* **20**, 2099 (1987).
27. C. M. Carter, J. C. Facelli, D. W. Alderman, D. M. Grant, N. K. Dalley, and B. E. Wilson, *J. Chem. Soc. Faraday Trans. I* **84**, 3673 (1988).
28. K. Schmidt-Rohr, M. Wilhelm, A. Johansson, and H. W. Spiess, *J. Chem. Phys.* **97**, 2247 (1992).
29. C. D. Hughes, M. H. Sherwood, D. W. Alderman, and D. M. Grant, *J. Magn. Reson. A* **102**, 58 (1993).
30. B. M. Fung and J. Afzal, *J. Am. Chem. Soc.* **108**, 1107 (1986).
31. C. Poon, J. Afzal, M. Gangoda, and B. M. Fung, *Magn. Reson. Chem.* **24**, 1014 (1986).